

# Angular distribution in $s$ -channel formation of the pentaquark $\Theta^+$ baryon

DIANA Collaboration

V.V. Barmin<sup>1</sup>, A.E. Asratyan<sup>1\*</sup>, C. Curceanu<sup>2</sup>, G.V. Davidenko<sup>1</sup>,  
C. Guaraldo<sup>2</sup>, M.A. Kubantsev<sup>1</sup>, I.F. Larin<sup>1</sup>, V.A. Matveev<sup>1</sup>,  
V.A. Shebanov<sup>1</sup>, N.N. Shishov<sup>1</sup>, L.I. Sokolov<sup>1</sup>, and V.V. Tarasov<sup>1</sup>

<sup>1</sup> *National Research Center Kurchatov Institute, Institute of Theoretical and Experimental Physics, ul. B. Chermushkinskaya 25, Moscow, 117218 Russia*

<sup>2</sup> *Laboratori Nazionali di Frascati dell' INFN, C.P. 13-I-00044 Frascati, Italy*

July 14, 2019

## Abstract

Using the DIANA data on the charge-exchange reaction  $K^+n \rightarrow pK^0$  on a bound neutron, in which the  $s$ -channel formation of the pentaquark baryon  $\Theta^+(1538)$  has been observed, we analyze the dependence of the background-subtracted  $\Theta^+ \rightarrow pK^0$  signal on the  $K^0$  emission angle in the  $pK^0$  rest frame. In order to describe the observed  $\cos \Theta_K^{\text{cms}}$  distribution, invoking the interference between the nonresonant  $s$ -wave and the  $\Theta^+$ -mediated higher-wave contributions to the amplitude of the charge-exchange reaction is required at a  $2.8\sigma$  level. The spin-parity assignment of  $1/2^-$  for the  $\Theta^+$  baryon is ruled out at a statistical level of 2.9 standard deviations. A selection in  $\cos \Theta_K^{\text{cms}}$  based on the observed angular dependence of the  $\Theta^+ \rightarrow pK^0$  signal allows to boost the statistical significance of the signal up to 7.1 standard deviations. This is far in excess of previously reported signals and renders the  $\Theta^+$  existence more credible.

PACS number(s): 13.75.Jz, 25.80.Nv

---

\*Corresponding author. E-mail address: ashot.asratyan@gmail.com

The exotic baryons with minimum quark configuration of  $(4q)\bar{q}$  have been theoretically discussed ever since the emergence of the quark model [1]. For such objects formed of light quarks, the lowest  $SU(3)$  representation was identified as the anti-decuplet that involves a single state with positive strangeness — the isosinglet baryon  $\Theta^+(uudd\bar{s})$ . This pentaquark baryon can be uniquely identified by the  $KN$  decays ( $K^+n$  and  $K^0p$ ) that are forbidden for the three-quark baryons. Since the “fall-apart” mechanism is not suppressed by any obvious selection rules, the decay width of the  $\Theta^+$  baryon was phenomenologically assumed to be rather big ( $\Gamma \sim 100$  MeV). The first rigorous predictions for the anti-decuplet of light pentaquark baryons were formulated in the landmark analysis [2] based on the chiral quark-soliton model. According to these theoretical predictions, the anti-decuplet baryons have spin-parity of  $1/2^+$ , and the mass of the isosinglet  $\Theta^+$  baryon should be close to 1530 MeV. The predicted decay width of the  $\Theta^+$  proved to be far below the earlier phenomenological estimates:  $\Gamma < 15$  MeV. Subsequently, some theorists using different assumptions came to a conclusion that the  $\Theta^+$  decay width should be well below this upper limit — on the order of 1 MeV or even less [3].

Narrow peaks near 1540 MeV in the effective-mass spectra of the systems  $nK^+$  and  $pK^0$  were initially observed in the reaction  $\gamma n \rightarrow nK^+K^-$  on the  $^{12}\text{C}$  nucleus in the LEPS experiment [4], and in the charge-exchange reaction  $K^+n \rightarrow pK^0$  on the Xe nucleus in the DIANA experiment [5]. Subsequently, both experiments confirmed their initial observations [6, 7, 8, 9]. Using the dynamics of  $s$ -channel formation of the  $\Theta^+$  in the charge-exchange reaction  $K^+n \rightarrow pK^0$ , DIANA was able to directly probe the  $\Theta^+$  decay width:  $\Gamma = 0.34 \pm 0.10$  MeV assuming  $J = 1/2$ . Other searches for the  $\Theta^+$  baryon in different reactions and experimental conditions yielded both positive and negative results, see the review papers [10, 11, 12]. A number of experimental groups have reneged on their initial positive evidence, that anyway was statistically insignificant and may have resulted from wishful thinking and the so-called “bandwagon effect”. Of the many null results, only a few that have been formulated in terms of the  $\Theta^+$  intrinsic width should be treated as physically meaningful. The best (albeit model-dependent) null result has been reported by the E19 experiment at J-PARC, where the  $\Theta^+$  signal was searched for in the  $K^-$  missing mass in the hadronic reaction  $\pi^-p \rightarrow K^-X$  [13]. The E19 upper limit on the  $\Theta^+$  decay width,  $\Gamma < 0.36$  MeV assuming the  $\Theta^+$  spin-parity of  $1/2^+$ , is narrowly consistent with the DIANA measurement. On the other hand, a group from the CLAS collaboration has recently re-analyzed their data for the reaction  $\gamma p \rightarrow K_S^0 K_L^0 p$  on hydrogen, invoking the interference between  $\phi p$  and  $\Theta^+ \bar{K}^0$  in the final state  $pK_L^0 K_S^0$

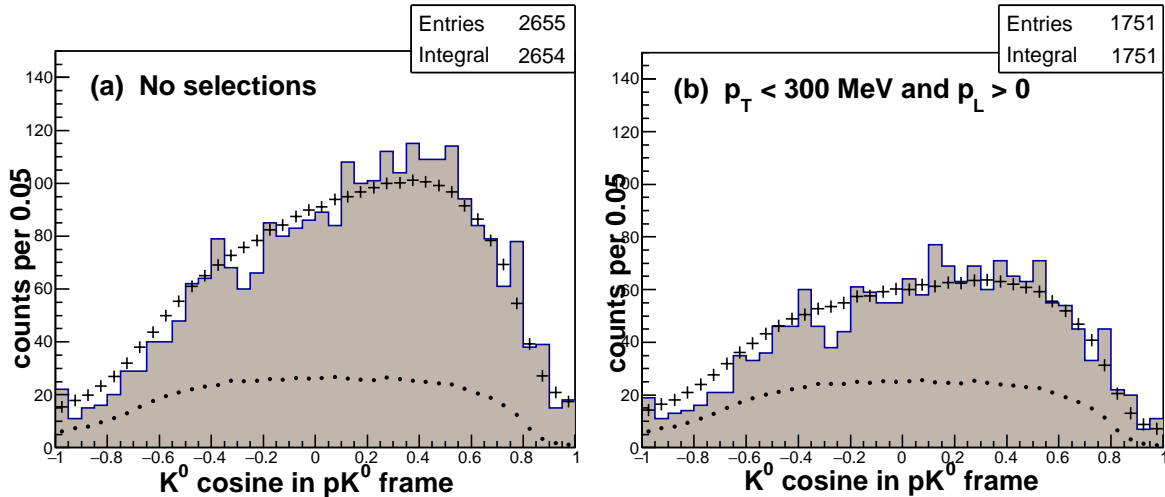


Figure 1: The cosine of the  $K^0$  emission angle in the  $pK^0$  rest frame,  $\Theta_{K^0}^{\text{cms}}$ , for all measured events (a) and upon applying the selections  $p_T < 300$  MeV and  $p_L > 0$  (b). The corresponding distributions of simulated events are shown by crosses, and the contributions of rescattering-free events — by dots.

[14]. A narrow statistically-significant peak near 1540 MeV, tentatively interpreted as the  $\Theta^+$  signal, has been observed in the  $K_S^0$  missing-mass spectrum. This observation does not contradict the null result earlier reported by CLAS for the same data sample [15].

In this paper, we continue the investigation of  $\Theta^+$  formation in the charge-exchange reaction  $K^+n \rightarrow pK^0$  on a bound neutron using the data of the DIANA experiment. In particular, we probe the angular distribution of decay products in the  $\Theta^+$  rest frame.

The DIANA bubble chamber filled with liquid Xenon was exposed to a separated beam of monochromatic  $K^+$  mesons from the 10-GeV proton synchrotron at ITEP, Moscow. In the fiducial volume of the bubble chamber,  $K^+$  momentum varies from  $\sim 730$  MeV for entering kaons to zero for those that range out through ionization. Throughout this momentum interval, all collisions and decays of incident  $K^+$  mesons are efficiently detected. The  $K^+$  momentum at interaction point is determined from the spatial distance between the detected vertex and the mean position of the vertices due to decays of stopping  $K^+$  mesons. Charged secondaries (electrons, pions, kaons, and protons) are identified by ionization and by decays at rest for kaons, and momentum-analyzed by their range in Xenon. The detection efficiency for  $\gamma$ -quanta with  $p_\gamma > 25$  MeV is close to 100%. Secondary  $K^0$  mesons are identified by the detectable decays  $K_S^0 \rightarrow \pi^+\pi^-$  and  $K_S^0 \rightarrow \pi^0\pi^0$ , and momentum-analyzed using the kinematic reconstruction. (In this analysis, only the former decay is used.) Further details on the experimental procedure may

be found in [9] and references therein. The candidate events for the charge-exchange reaction  $K^+n \rightarrow K^0p$  with no intranuclear rescatterings are selected as final states with a single proton and a  $K_S^0 \rightarrow \pi^+\pi^-$  decay. The instrumental thresholds for the momenta of secondary particles are  $p_K > 155$  MeV and  $p_p > 165$  MeV. The experimental resolution is near 3.5 MeV for the  $pK^0$  effective mass.

Plotted in Fig. 1(a) for all measured events is the cosine of the  $K^0$  emission angle in the  $pK^0$  rest frame with respect to the  $pK^0$  direction of motion,  $\cos \Theta_K^{\text{cms}}$ . Also shown is the  $\cos \Theta_K^{\text{cms}}$  distribution of all simulated  $pK^0$  events (crosses) and of those in which the proton and the  $K^0$  suffered no intranuclear rescatterings (dots). The former has been normalized to the number of all measured  $pK^0$  events. The effect of the selections in the transverse and longitudinal momenta of the  $pK^0$  system,  $p_T < 300$  MeV and  $p_L > 0$ , is shown in Fig. 1(b). These are seen to reject the rescattered events rather than the unrescattered ones. The simulation procedure has been described in [9].

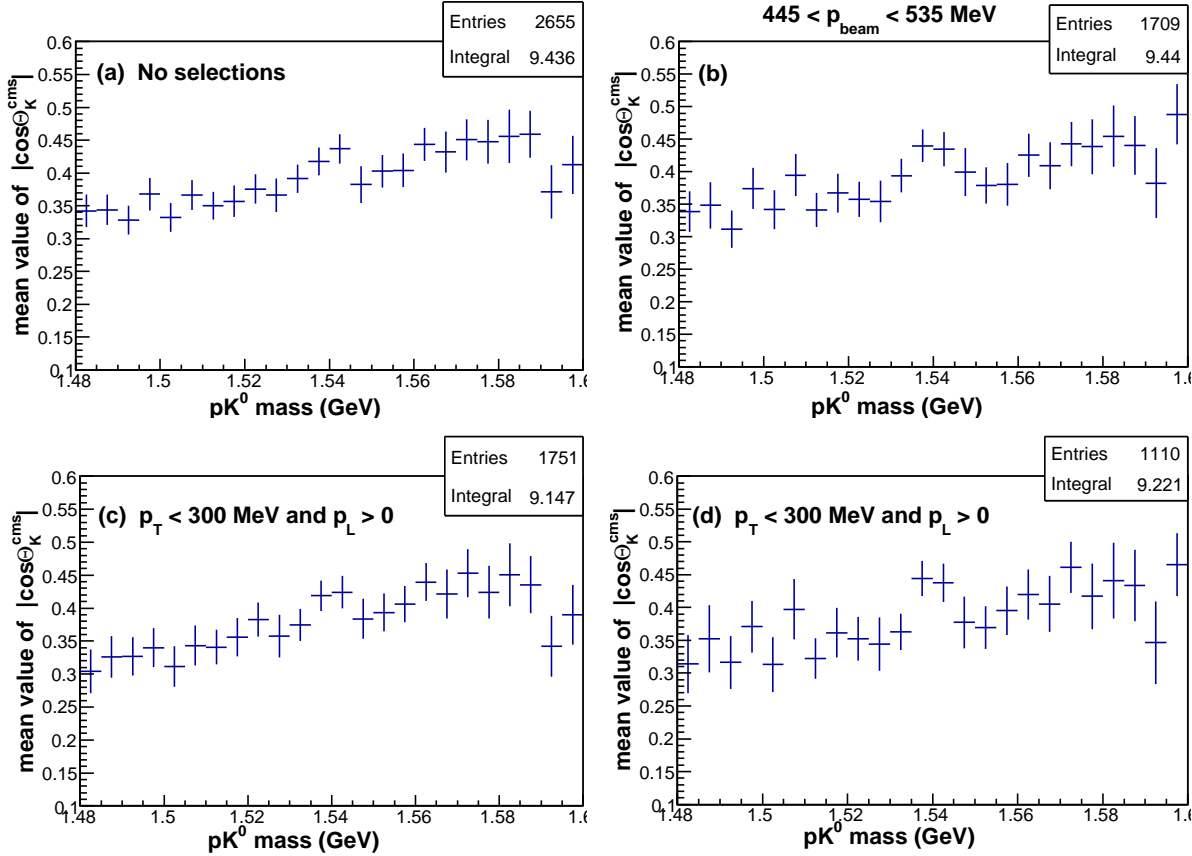


Figure 2: The mean value of  $|\cos \Theta_K^{\text{cms}}|$  as a function of the  $pK^0$  effective mass for all measured events (a) and for those in the region  $445 < p_{\text{beam}} < 535$  MeV (b). The effect of the selections  $p_T < 300$  MeV and  $p_L > 0$  is shown in (c) and (d).

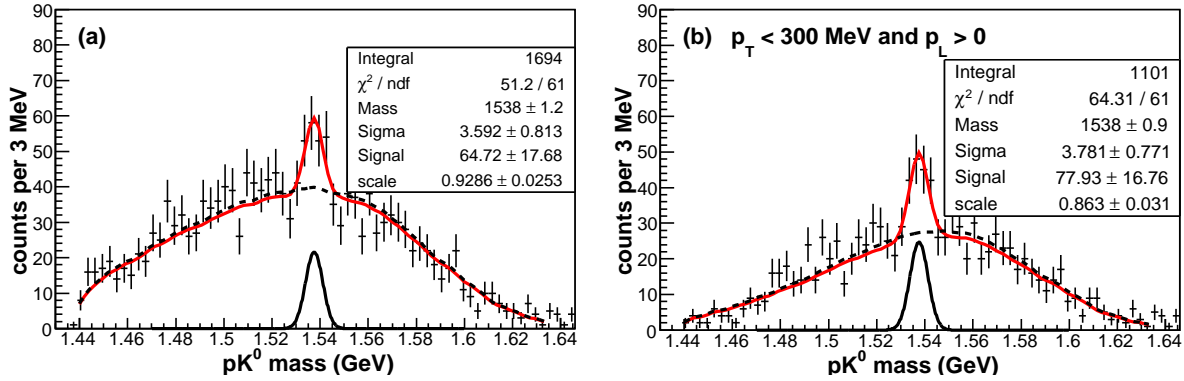


Figure 3: The  $pK^0$  effective mass prior to (a) and upon (b) applying the selections  $p_T < 300$  MeV and  $p_L > 0$ . Either mass spectrum is fitted to the simulated nonresonant background with variable normalization plus a Gaussian with variable position, width, and magnitude. The null fits to the background form alone are shown by dashed lines.

The mean value of  $|\cos \Theta_K^{\text{cms}}|$  is plotted in Fig. 2 as a function of the  $pK^0$  effective mass. The enhancement observed at  $m(pK^0) \simeq 1540$  MeV is emphasized by the selection in the  $K^+$  momentum at interaction point,  $445 < p_{\text{beam}} < 535$  MeV, that reflects the dynamics of  $s$ -channel formation of the  $\Theta^+$  baryon in the reaction  $K^+n \rightarrow pK^0$  on a bound neutron [9]. It is further emphasized by the selections  $p_T < 300$  MeV and  $p_L > 0$  aimed at rejecting the rescattered events. That the anomaly in  $|\cos \Theta_K^{\text{cms}}|$  occurs in the mass region of the observed  $\Theta^+$  peak [9] suggests that it is rooted in an “anomalous” angular distribution of  $\Theta^+$  decays that may show a quadratic term in  $\cos \Theta_K^{\text{cms}}$ . Therefore, it is interesting to compare the  $\cos \Theta_K^{\text{cms}}$  distribution for the mass region of the peak with that for the sideband areas of  $m(pK^0)$ . Except for the scatter plots discussed in the last paragraph, the selection  $445 < p_{\text{beam}} < 535$  MeV is implicitly assumed throughout.

The distribution of the  $pK^0$  effective mass is shown in Fig. 3(a), and upon applying the selections  $p_T < 300$  MeV and  $p_L > 0$  — in Fig. 3(b). Either mass spectrum is then fitted to the simulated nonresonant background with variable normalization plus a Gaussian with variable position, width, and magnitude. The width of the observed  $\Theta^+$  peak near 1538 MeV is consistent with the experimental resolution of  $\sigma_m \simeq 3.5$  MeV. In agreement with the fitted width of the  $\Theta^+$  signal, the peak area of the  $pK^0$  effective mass is selected as  $1530 < m(pK^0) < 1546$  MeV, and the sideband areas — as  $1514 < m(pK^0) < 1530$  MeV and  $1546 < m(pK^0) < 1562$  MeV. The  $\cos \Theta_K^{\text{cms}}$  distributions of events in the peak and sideband areas are shown in Figs. 4(a) and 4(c), respectively. The effect of the selections  $p_T < 300$  MeV and  $p_L > 0$  is shown in the corresponding right-

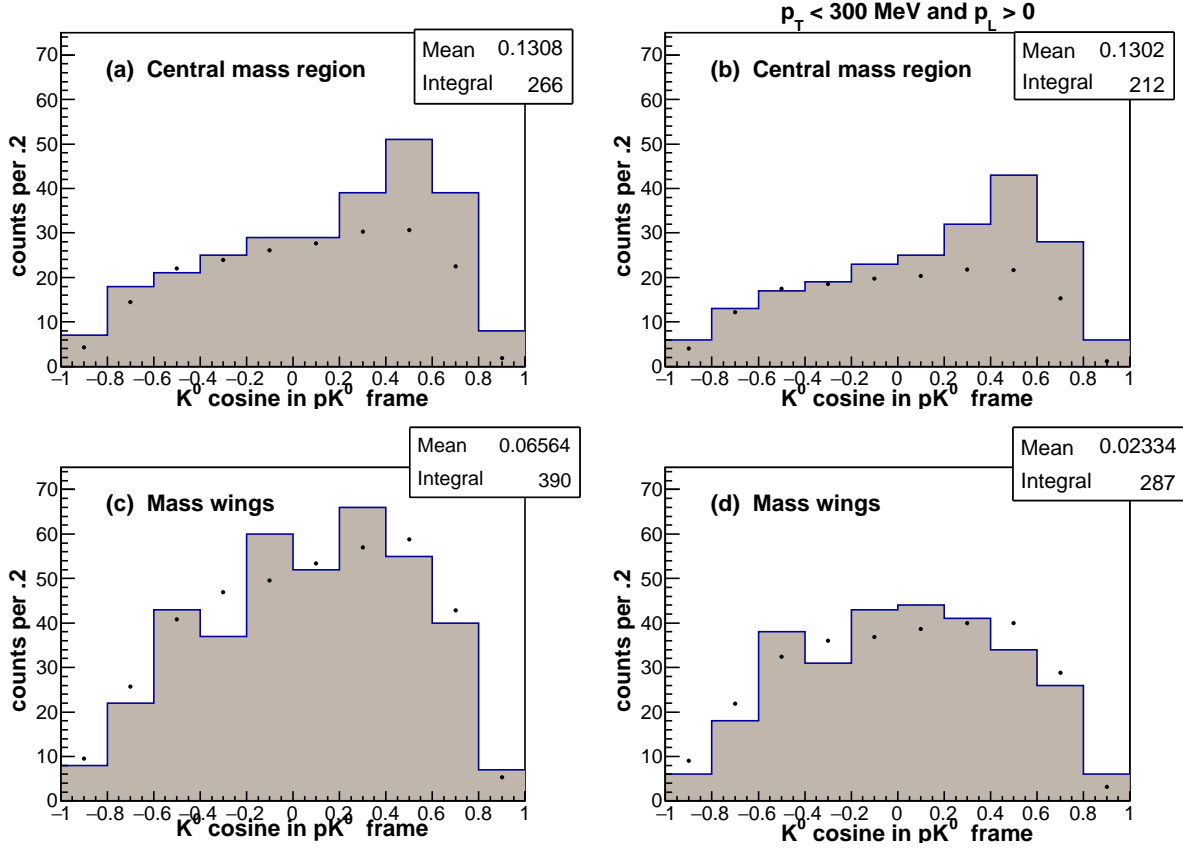


Figure 4: The  $\cos \Theta_K^{\text{cms}}$  distributions for the  $\Theta^+$  mass region of  $1530 < m(pK^0) < 1546$  MeV (a) and for the sideband regions of  $1514 < m(pK^0) < 1530$  MeV and  $1546 < m(pK^0) < 1562$  MeV (c). The effects of the selections  $p_T < 300$  MeV and  $p_L > 0$  are shown in (b) and (d). The simulated distributions are depicted by dots.

hand panels. For the sideband areas, the simulated distribution (dots) is normalized to the observed one by the number of events. Then, the same scaling factor is applied to the simulated  $\cos \Theta_K^{\text{cms}}$  distribution for the peak area. (As a result, there the simulated  $\cos \Theta_K^{\text{cms}}$  spectrum runs lower than the observed one.) The simulation that assumes a pure  $s$ -wave for the nonresonant reaction  $K^+n \rightarrow pK^0$  [16] agrees with the data for the sideband areas, but not for the peak area.

In order to obtain the “pure”  $\cos \Theta_K^{\text{cms}}$  spectrum for the decay  $\Theta^+ \rightarrow pK^0$ , we subtract the (halved)  $\cos \Theta_K^{\text{cms}}$  distribution for the sidebands from that for the  $\Theta^+$  peak region. Under the selections  $p_T < 300$  MeV and  $p_L > 0$  that reject nearly a half of the rescattered events, the sideband-subtracted  $\cos \Theta_K^{\text{cms}}$  spectrum is shown in Fig. 5. It is then compared with Monte-Carlo predictions for the  $\Theta^+$  formation and decay assuming the angular distribution in the forms  $dW/d \cos \Theta_K^{\text{cms}} \sim \text{const.}$  and  $dW/d \cos \Theta_K^{\text{cms}} \sim \cos^2 \Theta_K^{\text{cms}}$  as shown in Figs. 5(a) and 5(b), where the simulated distributions have been scaled to

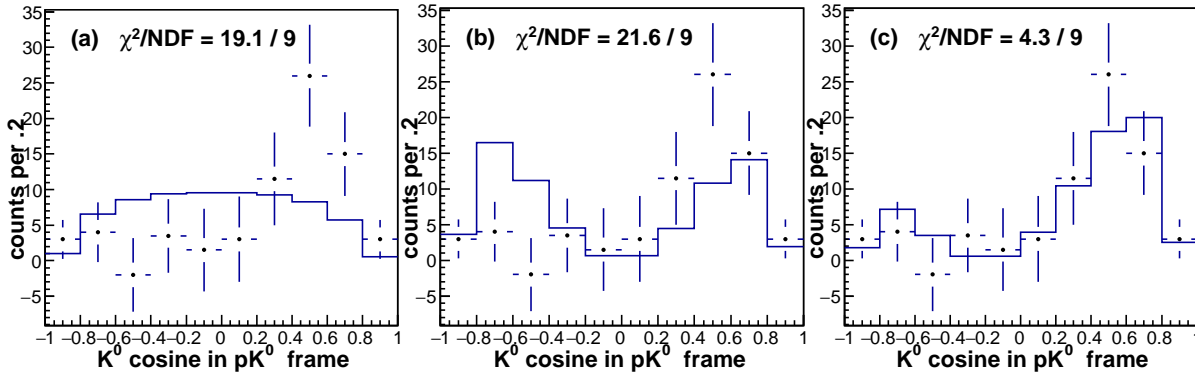


Figure 5: Under the selections  $p_T < 300$  MeV and  $p_L > 0$ , the sideband-subtracted  $\cos \Theta_K^{\text{cms}}$  distribution for the  $\Theta^+$  mass region compared with Monte-Carlo predictions for the  $\Theta^+$  decay angular distribution in the assumed forms  $dW/d\cos \Theta_K^{\text{cms}} \sim \text{const.}$  (a),  $dW/d\cos \Theta_K^{\text{cms}} \sim \cos^2 \Theta_K^{\text{cms}}$  (b), and  $dW/d\cos \Theta_K^{\text{cms}} \sim (\cos \Theta_K^{\text{cms}} + a)^2 + b$  with  $a = +0.2$  and  $b = 0$  (c). The simulated distributions have been scaled to the data by area.

the data by area. These forms are the two allowed components of the  $\cos \Theta_K^{\text{cms}}$  spectrum for arbitrary spin-parity of the decaying  $\Theta^+$  baryon. For both hypotheses, the values of  $\chi^2/\text{ndf}$  (19.1/9 and 21.6/9) are unacceptably high. We have also verified numerically that any linear combination of the above forms of the  $\cos \Theta_K^{\text{cms}}$  distribution for the decay  $\Theta^+ \rightarrow pK^0$  leads to  $\chi^2$  values in excess of 19 when compared with the observed sideband-subtracted  $\cos \Theta_K^{\text{cms}}$  spectrum.

In order to verify the conclusions reached with the  $\chi^2$  analysis of our low-statistics data, we also use the likelihood criterion. The likelihood function is constructed as a sum

$$-2 \ln L = 2 \sum_{i=1}^{10} \left[ -n_i + \nu_i + h_i + n_i \ln \frac{n_i}{\nu_i + h_i} \right],$$

where  $n_i$  and  $\nu_i$  are the bin contents of the experimental and simulated  $\cos \Theta_K^{\text{cms}}$  distributions for the  $\Theta^+$  central mass region shown in Fig. 4(b), and  $h_i$  are those of the simulated  $\cos \Theta_K^{\text{cms}}$  distribution for the given hypothesis of  $\Theta^+$  decay. The latter distribution has been scaled by the number of events to the difference between the former two, so that the fitting function as a whole is normalized to the observed  $\cos \Theta_K^{\text{cms}}$  distribution by area. For the hypotheses  $dW/d\cos \Theta_K^{\text{cms}} \sim \text{const.}$  and  $dW/d\cos \Theta_K^{\text{cms}} \sim \cos^2 \Theta_K^{\text{cms}}$ , we obtain  $-2 \ln L = 24.2$  and  $23.1$ , respectively. These values of  $-2 \ln L$  for  $\text{ndf} = 9$  correspond to the  $p$ -values near 0.005 and .007. As with the  $\chi^2$  analysis above, we find that assuming the  $\Theta^+$  decay angular distribution in the form of an arbitrary linear combination of the former two fails to tangibly reduce the value of  $-2 \ln L$ . This simple analysis sup-

ports the above conclusions based on the  $\chi^2$  criterion. From the derived  $p$ -values we may conclude that the uniform angular distribution  $dW/d\cos\Theta_K^{\text{cms}} \sim \text{const.}$  is inconsistent with the data at a statistical level of  $2.9\sigma$ , and the more general symmetric form  $dW/d\cos\Theta_K^{\text{cms}} \sim a + b\cos^2\Theta_K^{\text{cms}}$  — at a slightly lower level of  $2.8\sigma$ .

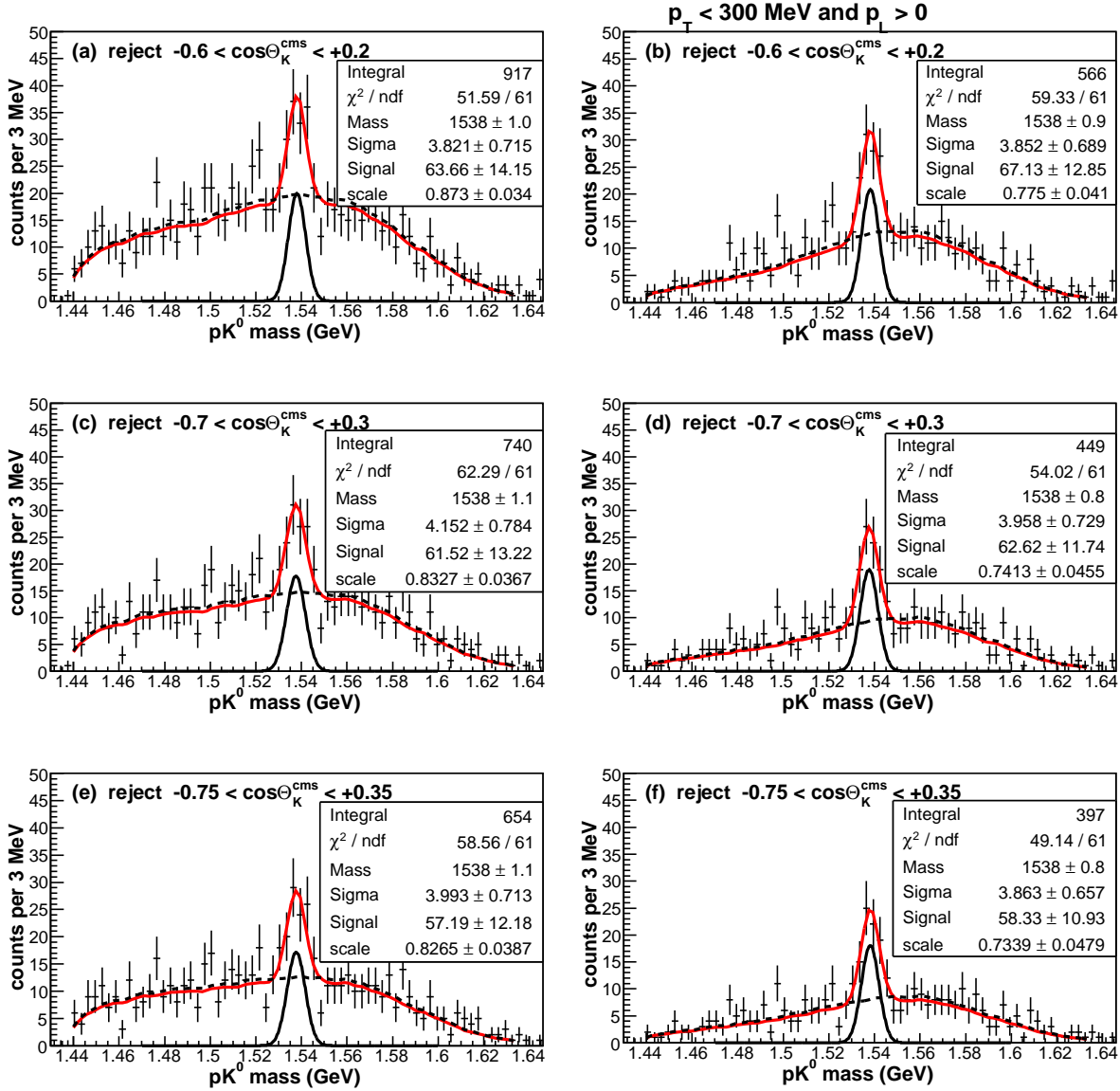


Figure 6: The  $pK^0$  effective-mass spectrum upon rejecting the events that fall within the  $\cos\Theta_K^{\text{cms}}$  intervals of  $-0.6 < \cos\Theta_K^{\text{cms}} < +0.2$  (a),  $-0.7 < \cos\Theta_K^{\text{cms}} < +0.3$  (c), and  $-0.75 < \cos\Theta_K^{\text{cms}} < +0.35$  (e). The effect of the selections  $p_T < 300 \text{ MeV}$  and  $p_L > 0$  is shown in the right-hand panels (b), (d), and (f). Each mass spectrum is fitted to the simulated nonresonant background with variable normalization plus a Gaussian with variable position, width, and magnitude. The null fits to the background form alone are shown by dashed lines.

The disagreement with any viable form of the  $\Theta^+$  decay angular distribution is rooted in the marked forward-backward asymmetry of the observed  $\cos \Theta_K^{\text{cms}}$  spectrum. The asymmetry in the form of a linear term in  $\cos \Theta_K^{\text{cms}}$ , required at a level of  $2.8\sigma$ , may arise only from the interference [17] between the nonresonant  $s$ -wave and the  $\Theta^+$ -mediated higher-wave contributions to the amplitude of the charge-exchange reaction  $K^+n \rightarrow pK^0$ . However, the interference should not affect the  $\cos \Theta_K^{\text{cms}}$  distribution for the signal as soon as the  $\Theta^+$  spin-parity is  $1/2^-$  implying an  $s$ -wave decay and a uniform  $\cos \Theta_K^{\text{cms}}$  distribution. Therefore, the  $1/2^-$  assignment is ruled out by the data at a level of 2.9 standard deviations.

The shape of the background-subtracted  $\Theta^+$  signal in Fig. 5 suggests an angular dependence of an asymmetric quadratic form  $dW/d \cos \Theta_K^{\text{cms}} \sim (\cos \Theta_K^{\text{cms}} + a)^2 + b$ , where  $b \simeq 0$  and the offset parameter  $a$  is positive at a  $2.8\sigma$  level. Tentatively substituting  $b = 0$  and  $a = +0.2$ , we obtain  $\chi^2/\text{ndf} = 4.3/9$  with the  $\chi^2$  approach as shown in Fig. 5(c), and  $-2 \ln L = 6.1$  for  $\text{ndf} = 9$  with the likelihood criterion which corresponds to a  $p$ -value near 0.8. (The assignments  $a = +0.1$  and  $a = +0.3$  also yield acceptable values of  $\chi^2$  and  $-2 \ln L$ .) The detailed interpretation of this form of the background-subtracted  $\cos \Theta_K^{\text{cms}}$  distribution requires a theoretical analysis of interference effects in terms of helicity amplitudes, and therefore is beyond the scope of this paper (apart from excluding the  $\Theta^+$  spin-parity assignment of  $1/2^-$ ). Instead, our major objective is to formulate a physically-reasonable data-driven selection that may render the  $\Theta^+$  signal more significant. This is an important task since the signals reported thus far [6, 9, 14] are but slightly in excess of  $5\sigma$ , whereas the ‘‘credibility threshold’’ for proving the  $\Theta^+$  existence has been estimated as  $7\sigma$  [18] given the controversial experimental situation.

If formation of the  $\Theta^+$  baryon indeed follows the distribution  $dW/d \cos \Theta_K^{\text{cms}} \sim (\cos \Theta_K^{\text{cms}} + a)^2 + b$  as argued above, rejecting the events with  $\cos \Theta_K^{\text{cms}}$  values near the minimum of the parabola at  $-a$  should enhance the signal-to-background ratio in the  $pK^0$  effective-mass spectrum and the statistical significance of the  $\Theta^+$  peak. Shown in Fig. 6 are the effects of cutting away the  $\cos \Theta_K^{\text{cms}}$  intervals centered on  $\cos \Theta_K^{\text{cms}} = -0.2$ :  $-0.6 < \cos \Theta_K^{\text{cms}} < +0.2$ ,  $-0.7 < \cos \Theta_K^{\text{cms}} < +0.3$ , and  $-0.75 < \cos \Theta_K^{\text{cms}} < +0.35$ . Each mass spectrum is again fitted to the simulated nonresonant background with variable normalization plus a Gaussian with variable position, width, and magnitude. The width of the observed  $\Theta^+$  peak is always consistent with the experimental resolution of  $\sigma_m \simeq 3.5$  MeV. Indeed, cutting on  $\cos \Theta_K^{\text{cms}}$  is seen to result in a dramatic increase of the signal-to-background ratio as compared to the  $pK^0$  mass spectra of Fig. 3.

Rejected $\cos \Theta_K^{\text{cms}}$ interval	$m_0$ (MeV)	Signal (ev) $S/\sqrt{B}$	$-\ln L$ $\chi^2/\text{ndf}$ (signal fit)	$-\ln L$ $\chi^2/\text{ndf}$ (null fit)	$2\Delta \ln L$	Stat. sign.
None	$1538 \pm 1$	$74.9 \pm 14.5$ 6.8	31.5 64.5/62	46.6 91.3/64	30.1	$5.1\sigma$
$-0.6 < \cos \Theta_K^{\text{cms}} < +0.2$	$1538 \pm 1$	$64.1 \pm 11.3$ 8.6	35.0 59.6/62	57.2 91.9/64	44.4	$6.3\sigma$
$-0.7 < \cos \Theta_K^{\text{cms}} < +0.3$	$1538 \pm 1$	$59.3 \pm 10.3$ 9.3	30.9 54.4/62	55.2 87.5/64	48.5	$6.6\sigma$
$-0.75 < \cos \Theta_K^{\text{cms}} < +0.35$	$1538 \pm 1$	$55.8 \pm 9.8$ 9.4	29.3 49.5/62	54.4 81.8/64	50.2	$6.8\sigma$

Table 1: The results of the fits of the  $pK^0$  mass spectra under the selections  $p_T < 300$  MeV and  $p_L > 0$ , in which the Gaussian width of the signal has been constrained to the simulated resolution of  $\sigma_m = 3.5$  MeV. The statistical significance of the signal, estimated using the method of maximum likelihood, is shown in the rightmost column. Also shown is the “naive” estimate of the statistical significance  $S/\sqrt{B}$ , where the signal  $S$  and the background  $B$  are derived from the signal hypothesis alone over the 90% area of the Gaussian.

In order to reduce the number of free parameters, the width of the peak is constrained to the simulated value of  $\sigma_m = 3.5$  MeV when estimating the statistical significance of the signal. The results of the constrained fits of the  $pK^0$  mass spectra under the selections  $p_T < 300$  MeV and  $p_L > 0$  are shown in Table 1. Also shown for each fit is the difference between the log-likelihood values for the signal and null hypotheses,  $-2\Delta \ln L$ . For the constrained fits, the numbers of degrees of freedom for the signal and null hypotheses differ by  $\Delta \text{ndf} = 2$ . The statistical significance of the signal is estimated using the value of  $\chi^2$  for one degree of freedom which corresponds to the same  $p$ -value as  $\chi^2 = -2\Delta \ln L$  for two degrees of freedom. Rejecting the central values of  $\cos \Theta_K^{\text{cms}}$  is seen to boost the statistical significance of the  $\Theta^+$  signal from  $5.1\sigma$  up to  $6.8\sigma$ . The “naive” estimate of the statistical significance reaches  $S/\sqrt{B} = 9.4\sigma$ , where the signal  $S$  and the background  $B$  have been derived from the signal fit alone over the 90% area of the Gaussian. That the significance of the  $\Theta^+$  signal is substantially increased by an asymmetric  $\cos \Theta_K^{\text{cms}}$  cut *a posteriori* indicates that both the quadratic and linear terms contribute to the  $\cos \Theta_K^{\text{cms}}$  distribution.

And finally, beam momentum  $p(K^+)$  is plotted versus the  $pK^0$  effective mass under the selections  $p_T < 300$  MeV and  $p_L > 0$  in Fig. 7(a), and upon rejecting the events with

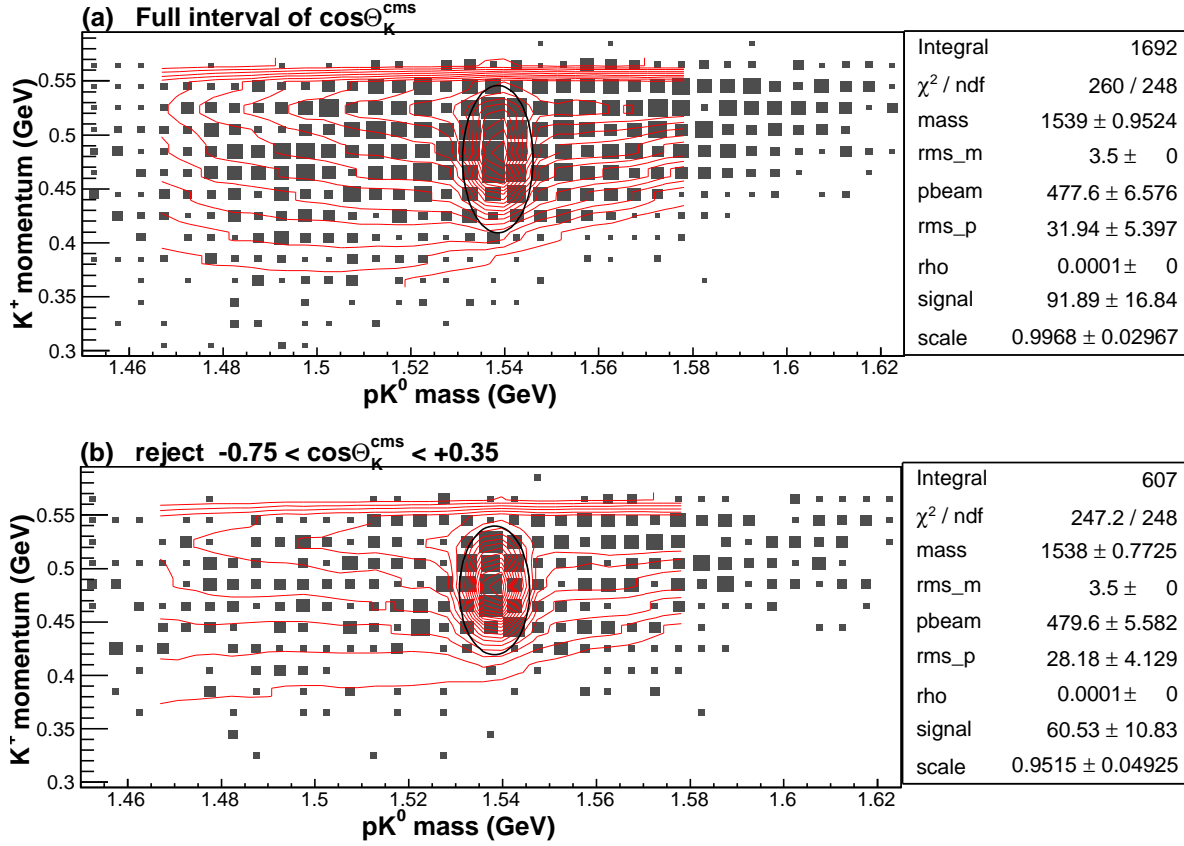


Figure 7: Under the selections  $p_T < 300$  MeV and  $p_L > 0$ , beam momentum  $p(K^+)$  plotted versus the  $pK^0$  effective mass (a). The effect of rejecting the events with  $-0.75 < \cos\Theta_K^{\text{cms}} < +0.35$  is shown in (b). Either scatter plot is fitted to the corresponding simulated distribution with variable normalization plus a two-dimensional Gaussian. The width of the Gaussian in  $m(pK^0)$  and the correlation parameter  $\rho$  have been constrained to the experimental mass resolution  $\sigma_m = 3.5$  MeV and to zero, respectively. The ellipses show the 90% areas of the Gaussians.

$-0.75 < \cos\Theta_K^{\text{cms}} < +0.35$  — in Fig. 7(b). The latter selection results in a distinct  $\Theta^+$  signal at expected values of  $m(pK^0)$  and  $p(K^+)$ . Either scatter plot is then fitted to the corresponding simulated distribution with variable normalization plus a two-dimensional Gaussian. The width of the Gaussian in  $m(pK^0)$  is constrained to the experimental mass resolution of  $\sigma_m = 3.5$  MeV, and the correlation parameter  $\rho$  is constrained to zero as physically expected for formation of a narrow resonance (as the observed mass should not depend on beam momentum). Either scatter plot has also been fitted to the background form alone (not shown). For the fits in Figs. 7(a) and 7(b), we have  $-2\Delta \ln L = 49.7$  and 61.9 for  $\Delta \text{ndf} = 4$ . The statistical significance of the signal is again estimated using the value of  $\chi^2$  for one degree of freedom which corresponds to the same  $p$ -value as  $\chi^2 = -2\Delta \ln L$  for four degrees of freedom. Thereby, we obtain that cutting away the

$\cos \Theta_K^{\text{cms}}$  region of  $-0.75 < \cos \Theta_K^{\text{cms}} < +0.35$  allows to increase the statistical significance of the  $\Theta^+ \rightarrow pK^0$  signal from  $6.2\sigma$  up to  $7.1\sigma$ .

In summary, using the data on the charge-exchange reaction  $K^+n \rightarrow pK^0$  on a bound neutron, we have analyzed the dependence of the background-subtracted  $\Theta^+ \rightarrow pK^0$  signal on the  $K^0$  emission angle in the  $pK^0$  rest frame,  $\Theta_K^{\text{cms}}$ . In order to describe the observed  $\cos \Theta_K^{\text{cms}}$  distribution, invoking the interference between the nonresonant  $s$ -wave and the  $\Theta^+$ -mediated higher-wave contributions to the amplitude of the charge-exchange reaction is required at a level of  $2.8\sigma$ . The spin-parity assignment of  $1/2^-$  for the  $\Theta^+$  baryon is ruled out at a statistical level of  $2.9\sigma$ . A selection in  $\cos \Theta_K^{\text{cms}}$  based on the observed angular dependence of the background-subtracted  $\Theta^+ \rightarrow pK^0$  signal allows to boost the statistical significance of the signal up to  $6.8\sigma$  for the one-dimensional  $pK^0$  mass spectrum, and  $7.1\sigma$  for the scatter plot in  $m(pK^0)$  and  $p(K^+)$ . This is far in excess of previously reported signals [6, 9, 14] and renders the  $\Theta^+$  existence more credible [18].

## References

- [1] M. Gell-Mann, Phys. Lett. 8, 214 (1964); R.L. Jaffe, Phys. Rev. D 15, 281 (1977); A.T.M. Aerts, P.J.G. Mulders, and J.J. de Swart, *ibid.* D 17, 260 (1978); M. de Crombrughe, H. Hogaasen, and P. Sorba, Nucl. Phys. B 156, 347 (1979).
- [2] D. Diakonov, V. Petrov, and M. Polyakov, Z. Phys. A 359, 305 (1997).
- [3] D. Diakonov and V. Petrov, Phys. Rev. D 72, 074009 (2005); C. Lorce, *ibid.* D 74, 054019 (2006); A.G. Oganesian, JETP Lett. 84, 409 (2006); Int. J. Mod. Phys. A 22, 2093 (2007); Hyun-Chul Kim, Tim Ledwig, and Klaus Goeke, Mod. Phys. Lett. A 23, 2238 (2008); Tim Ledwig, Hyun-Chul Kim, and Klaus Goeke, Phys. Rev. D 78, 054005 (2008); Nucl. Phys. A 811, 353 (2008).
- [4] T. Nakano, D.S. Ahn, J.K. Ahn et al. (LEPS Collaboration), Phys. Rev. Lett. 91, 012002 (2003).
- [5] V.V. Barmin, V.S. Borisov, G.V. Davidenko et al. (DIANA Collaboration), Yad. Fiz. 66, 1763 (2003) [Phys. Atom. Nucl. 66, 1715 (2003)].
- [6] T. Nakano, N. Muramatsu, D.S. Ahn et al. (LEPS Collaboration), Phys. Rev. C 79, 025210 (2009).

- [7] V.V. Barmin, A.E. Asratyan, V.S. Borisov et al. (DIANA Collaboration), *Yad. Fiz.* 70, 39 (2007) [*Phys. Atom. Nucl.* 70, 35 (2007)].
- [8] V.V. Barmin, A.E. Asratyan, V.S. Borisov et al. (DIANA Collaboration), *Yad. Fiz.* 73, 1 (2010) [*Phys. Atom. Nucl.* 73, 1168 (2010)].
- [9] V.V. Barmin, A.E. Asratyan, V.S. Borisov et al. (DIANA Collaboration), *Phys. Rev. C* 89, 045204 (2014).
- [10] Volker D. Burkert, *Int. J. Mod. Phys. A* 21, 1764 (2006).
- [11] M.V. Danilov and R.V. Mizuk, *Phys. Atom. Nucl.* 71, 605 (2008).
- [12] K.H. Hicks, *Eur. Phys. J. H* 37, 1 (2012).
- [13] M. Moritsu, S. Adachi, M. Agnello et al. (E19 Collaboration), *Phys. Rev. C* 90, 035205 (2014).
- [14] M.J. Amarian, G. Gavalian, C. Nepali et al., *Phys. Rev. C* 85, 035209 (2012).
- [15] R. De Vita, M. Battaglieri, V. Kubarovsky et al. (CLAS Collaboration), *Phys. Rev. D* 74, 032001 (2006).
- [16] C.B. Dover and G.E. Walker, *Phys. Rep.* 89, 1 (1982).
- [17] A. Sibirtsev, J. Haidenbauer, S. Krewald, and Ulf-G. Meissner, *Eur. Phys. J. A* 23, 491 (2005).
- [18] Louis Lions, arXiv:1310.1284 [physics.dat-an].